

Dynamical mean-field theory, density-matrix embedding theory, and rotationally invariant slave bosons: A unified perspective

Thomas Ayrál,¹ Tsung-Han Lee,¹ and Gabriel Kotliar^{1,2}

¹*Physics and Astronomy Department, Rutgers University, Piscataway, New Jersey 08854, USA*

²*Condensed Matter Physics and Materials Science Department, Brookhaven National Laboratory, Upton, New York 11973, USA*

(Received 21 October 2017; published 26 December 2017)

We present a unified perspective on dynamical mean-field theory (DMFT), density-matrix embedding theory (DMET), and rotationally invariant slave bosons (RISB). We show that DMET can be regarded as a simplification of the RISB method where the quasiparticle weight is set to unity. This relation makes it easy to transpose extensions of a given method to another: For instance, a temperature-dependent version of RISB can be used to derive a temperature-dependent free-energy formula for DMET.

DOI: [10.1103/PhysRevB.96.235139](https://doi.org/10.1103/PhysRevB.96.235139)

Strong correlations count among the most challenging problems in condensed-matter physics. While the development of dynamical mean-field theory (DMFT) [1] and its cluster [2–6] and diagrammatic [7] extensions has led to a better understanding of relatively simple, strongly correlated models and systems, there are still situations where the exact solution of the DMFT quantum impurity model becomes prohibitive due to the size of its Hilbert space and/or the Monte Carlo negative-sign problem. These situations range from the study of multiorbital systems to the exploration of low-temperature phases over the investigation of long-range strong correlations. This is particularly important for realistic investigations of $5f$ systems, which require the simultaneous inclusion of crystal-field effects, spin-orbit-coupling interaction multiplets, and lattice relaxation. Outstanding challenges in this area include the computation of phase diagrams and equations of state of elemental actinides and their alloys. These are problems of fundamental importance and of practical technological relevance, and they require simplified, fast methods that still capture correlation effects accurately enough.

Several such methods have been developed in recent years, with a commonality with DMFT: the mapping of the lattice problem onto a simpler, yet still nontrivial embedded quantum problem. Prominent examples include cluster perturbation theory (CPT [8,9], derivable from the self-energy functional theory, SFT [10,11]), self-energy embedding theory (SEET [12,13]), two-site DMFT [14,15], and site-occupation embedding theory (SOET [16,17]).

Two particularly successful methods are the (mean-field) rotationally invariant slave boson method (RISB [18,19]) and the density-matrix embedding theory (DMET [20,21]). RISB yields kinetic energy renormalizations, double occupancies, and valence histograms very close to those of DMFT [22–24] and has been applied to numerous multiband models [19,25–27] and realistic compounds [27–29]. These slave boson methods have a close connection to the Gutzwiller approximation as shown in Ref. [30] for the single-site case and in Ref. [31] for the multiorbital case. As for DMET, it has been shown to yield very accurate ground-state energies for the Hubbard model [20,21,32–34] and quantum chemical systems [35,36]. Both give access to ground-state (including superconducting [32,37,38]) properties and spectral properties [39], and have also been extended to tackle out-of-equilibrium problems [40–47].

However, the precise relation between these two methods has not been established to date and it is unclear whether they yield a complementary picture of correlations, or if on the contrary one corresponds to the simplification of the other. This work intends to fill this gap by showing that DMET is a simplification of RISB. We also illustrate the relation of RISB with DMFT, thereby giving a comprehensive picture of the interrelation and hierarchy between the three methods.

This paper is organized as follows: We first give an overview of the results presented in this paper (Sec. I), then review the RISB formalism and its relation with DMFT (Sec. II), and finally derive the DMET approximation and show that it is a simplified RISB with a quasiparticle weight equal to 1 (Sec. III).

I. OVERVIEW

In this section, we highlight the common structures of RISB and DMET without providing detailed derivations. Our purpose is to provide the reader with the key ideas that these methods share and thus reveal their close connection.

Both RISB and DMET start with an *interacting lattice model* of the form

$$\hat{H} = \sum_{ij,\alpha\beta} \tilde{t}_{i\alpha,j\beta} c_{i\alpha}^\dagger c_{j\beta} + \sum_i \hat{H}_{\text{loc}}[\{c_{i\alpha}, c_{i\alpha}^\dagger\}], \quad (1)$$

depicted in Fig. 1, top panel. Greek indices $\alpha, \beta, \dots = 1 \dots \mathcal{N}_c$ denote local or orbital indices (within a unit cell). Latin indices $i, j, \dots = 1 \dots \mathcal{N}/\mathcal{N}_c$ denote unit cells. (The local or orbital degrees of freedom may as well refer to inequivalent sites in a cellular-DMFT-like construction, so that a “unit cell” may also refer to a cluster cell). The first term is a kinetic term describing hopping processes between different unit cells. The hopping \tilde{t} does not contain local hopping terms ($\tilde{t}_{i\alpha,i\beta} = 0$); instead, they are contained in \hat{H}_{loc} . Later, we will denote by t the full hopping matrix and by \hat{H}_{int} the interaction Hamiltonian (without local hoppings).

The key idea of RISB and DMET is to replace the lattice model by a reference model or *effective medium* that depicts correlations in an approximate fashion.

In DMET, this effective medium consists of one correlated unit cell, called the *fragment*, and an *environment* where the effect of correlations is described by a one-body potential λ , as illustrated in Fig. 1, middle panel. (In the DMET literature,

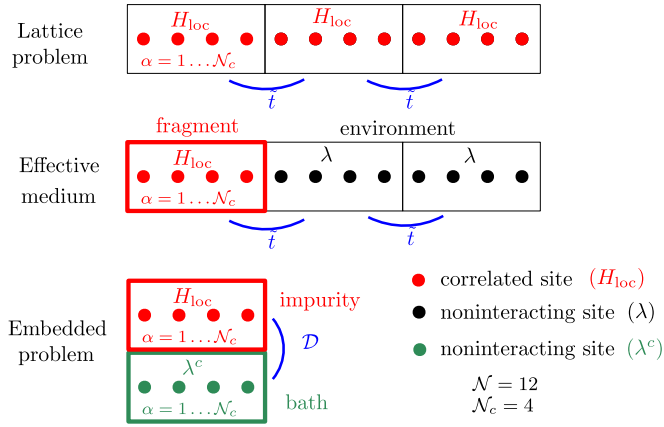


FIG. 1. Three layers of RISB and DMET. *Top*: Lattice problem: all unit cells are interacting. *Middle*: Effective medium: only the unit cell dubbed “fragment” is interacting, correlations for the rest (“environment”) are described by a one-body potential λ . *Bottom*: Embedded problem: the environment is mapped to a “bath” of the same dimension as the fragment/impurity.

this potential is usually called u and is equal to λ up to a local hopping term: $\lambda_{\alpha\beta} = u_{\alpha\beta} + [\varepsilon_{\text{loc}}]_{\alpha\beta}$.) The Hamiltonian of this effective medium is

$$\hat{H}_{\text{eff}} \equiv \sum_{ij,\alpha\beta} \tilde{t}_{i\alpha,j\beta} c_{i\alpha}^\dagger c_{j\beta} + \hat{H}_{\text{loc}}[\{c_{0\alpha}, c_{0\alpha}^\dagger\}] + \sum_{i \neq 0, \alpha\beta} \lambda_{\alpha\beta} c_{i\alpha}^\dagger c_{i\beta}. \quad (2)$$

RISB also has an effective medium, but it comes with an additional parameter (called R in the following) that is used to describe the mass of quasiparticles. This medium cannot be described by a one-body potential only.

As a last step, both methods introduce an impurity or *embedded problem* illustrated in Fig. 1, bottom panel. It is obtained by the contraction of the environment (of size $\mathcal{N} - \mathcal{N}_c$) to \mathcal{N}_c bath orbitals using a Schmidt decomposition. The embedded problem thus consists of \mathcal{N}_c correlated or *impurity* orbitals hybridized (via a hybridization term \mathcal{D}) to \mathcal{N}_c uncorrelated bath orbitals (described by the one-body potential λ^c). It is given by a Hamiltonian of the form

$$\begin{aligned}
 \hat{H}_{\text{embed}} \equiv & \sum_{\alpha\beta} (\mathcal{D}_{\alpha\beta} c_\alpha^\dagger a_\beta + \text{H.c.}) + \hat{H}_{\text{loc}}[\{c_\alpha^\dagger, c_\alpha\}] \\
 & + \sum_{\alpha\beta} \lambda_{\alpha\beta}^c a_\beta a_\alpha^\dagger. \quad (3)
 \end{aligned}$$

Here, c^\dagger and c (respectively, a^\dagger and a) are creation and annihilation operators for the impurity (resp., bath) orbitals.

The goal of both methods is to determine the effective medium, i.e., to find the value of λ (and optionally R), such that the following self-consistency condition is satisfied: The one-particle *density matrix* of the impurity model [Eq. (3)] must match the projection of the reference medium’s density matrix onto the embedded subspace. λ (and optionally R) can then be used to construct approximations to the self-energy of the lattice model.

This is also the logic of DMFT, except that DMFT adjusts the local self-energy $\Sigma_{\text{loc}}(i\omega)$ (instead of λ and R above) so

that the (one-particle) Green’s function,

$$[G_{\text{imp}}]_{\alpha\beta}(i\omega_n) \equiv - \int_0^\beta d\tau e^{i\omega_n\tau} \langle T c_\alpha(\tau) c_\beta^\dagger(0) \rangle_{\text{imp}}, \quad (4)$$

of the impurity model matches the projection of the reference medium’s Green’s function,

$$G(\mathbf{k}, i\omega) = [i\omega - \varepsilon_{\mathbf{k}} - \Sigma_{\text{loc}}(i\omega)]^{-1}, \quad (5)$$

onto the impurity [where $\varepsilon_{\mathbf{k}}$ is the Fourier transform of the hopping matrix t_{ij} or local density approximation (LDA) Hamiltonian in a LDA+DMFT context; see Eq. (7) below]. Besides, because of this modified self-consistency condition, the impurity model of DMFT contains an infinite number of bath sites, contrary to Eq. (3).

While connections among RISB, DMET, and DMFT have been mentioned in passing (see, e.g., Ref. [28]) and DMET was inspired by DMFT, a precise direct connection has not been available in the literature to date. This connection points to many possible generalizations of these methods.

II. OVERVIEW OF ROTATIONALLY INVARIANT SLAVE BOSONS

In this section, we briefly review the RISB formalism introduced by Ref. [19]. Our starting point is the lattice Hamiltonian Eq. (1). We note that \hat{H}_{loc} contains both kinetic and interaction terms. Denoting by $t_{i\alpha,j\beta}$ hoppings internal to a unit cell, we can decompose

$$\begin{aligned}
 \hat{H}_{\text{loc}} &= \hat{H}_{\text{int}} + \sum_i \sum_{\alpha\beta} t_{i\alpha,i\beta} c_{i\alpha}^\dagger c_{i\beta}, \\
 \tilde{t}_{i\alpha,j\beta} &= \begin{cases} t_{i\alpha,j\beta} & \text{if } i \neq j \\ 0 & \text{otherwise} \end{cases}. \quad (6)
 \end{aligned}$$

In the following, we will denote the i, j Fourier transform of $t_{i\alpha,j\beta}$ (resp., $\tilde{t}_{i\alpha,j\beta}$) as

$$\varepsilon_{\mathbf{k},\alpha\beta} \equiv \frac{\mathcal{N}_c}{\mathcal{N}} \sum_{ij} e^{-i\mathbf{k}\cdot(\mathbf{r}_i - \mathbf{r}_j)} t_{i\alpha,j\beta} \quad (7)$$

(resp., $\tilde{\varepsilon}_{\mathbf{k},\alpha\beta}$). Correspondingly,

$$[\varepsilon_{\text{loc}}]_{\alpha\beta} \equiv \sum_{\mathbf{k}} \varepsilon_{\mathbf{k},\alpha\beta} = t_{0\alpha,0\beta}. \quad (8)$$

A. Slave bosons: Constraints and physical subspace

The second-quantized operators $c_{i\alpha}^\dagger, c_{i\alpha}$ generate a Hilbert space $\mathcal{H}_{\text{phys}}$ with *local* many body states $|A_i\rangle$. RISB consists in introducing fermionic operators $f_{i\alpha}^\dagger, f_{i\alpha}$ and bosonic operators $\hat{\phi}_{A_i,n_i}^\dagger, \hat{\phi}_{A_i,n_i}$ (one for each *pair* of *local* many-body states, with n_i labeling local Fock states, which like A_i form a basis of the local Hilbert space) to replace c^\dagger and c . Yet, these new operators generate a Hilbert space \mathcal{H} which is much larger than the original Hilbert space, so that one needs to define a “physical” subspace. This is done by defining *physical states* and the corresponding *constraints*. The physical states are defined as follows:

$$|\underline{A}_i\rangle \equiv \frac{1}{\sqrt{D_A}} \sum_{n_i} \hat{\phi}_{A_i,n_i}^\dagger |0\rangle |n_i\rangle_f, \quad (9)$$

with $D_A \equiv \binom{\mathcal{N}_c}{\mathcal{N}_A}$ (\mathcal{N}_A is the number of electrons in state A) and the $\{|n_i\rangle_f\}$ are the local Fock states formed with f^\dagger operators:

$$|n_i\rangle_f \equiv \prod_{\alpha=1}^{\mathcal{N}_c} (f_{i\alpha}^\dagger)^{n_{i\alpha}} |0\rangle. \quad (10)$$

One can check that the physical states $|\underline{A}_i\rangle$ are normalized. One can prove [19] that these states (and only these states) satisfy the following constraints:

$$\forall i \sum_{A_i n_i} \hat{\phi}_{A_i n_i}^\dagger \hat{\phi}_{A_i n_i} = 1, \quad (11a)$$

$$\forall i, \alpha, \beta \quad f_{i\alpha}^\dagger f_{i\beta} = \sum_{A_i n_i m_i} f(m_i | f_{i\alpha}^\dagger f_{i\beta} | n_i)_f \hat{\phi}_{A_i n_i}^\dagger \hat{\phi}_{A_i m_i}. \quad (11b)$$

In the following, we drop the site index i for conciseness.

One then writes a *faithful representation* of the original Hamiltonian H in the physical subspace, where “faithful” is defined as follows: For any (local) operator O , \underline{O} is said to be a faithful representation of O in the physical subspace if and only if

$$\forall A, B, \quad \langle \underline{A} | \underline{O} | \underline{B} \rangle = \langle A | O | B \rangle. \quad (12)$$

One can show [19] that the faithful representation of the creation operator is given by the expression

$$\underline{c}_\alpha^\dagger = \sum_\beta R_{\beta\alpha} f_\beta^\dagger, \quad (13)$$

with the $\hat{\phi}$ -dependent matrix R defined by

$$R_{\beta\alpha} \equiv \sum_{ABnm} \frac{\langle A | c_\alpha^\dagger | B \rangle_f \langle n | f_\beta^\dagger | m \rangle_f}{\sqrt{\mathcal{N}_A(\mathcal{N}_c - \mathcal{N}_B)}} \hat{\phi}_{An}^\dagger \hat{\phi}_{Bm}. \quad (14)$$

Equation (13) is used to write down the faithful representation of the kinetic term of the Hamiltonian. For the local Hamiltonian term (which contains interactions and local hoppings, see above), one can show [19] that

$$\underline{H}_{\text{loc}} = \sum_{iABn} \langle A_i | H_{\text{loc}} | B_i \rangle \hat{\phi}_{A_i n_i}^\dagger \hat{\phi}_{B_i n_i}. \quad (15)$$

One can thus write the faithful representation of H in terms of the f and $\hat{\phi}$ fields:

$$\begin{aligned} \underline{H} = & \sum_{ij, \gamma\delta} \left\{ \sum_{\alpha\beta} R_{\gamma\alpha} \tilde{t}_{i\alpha, j\beta} R_{\beta\delta}^\dagger \right\} f_{i\gamma}^\dagger f_{j\delta} \\ & + \sum_{i, AB} \langle A_i | H_{\text{loc}} | B_i \rangle \sum_{n_i} \hat{\phi}_{A_i n_i}^\dagger \hat{\phi}_{B_i n_i}. \end{aligned} \quad (16)$$

This Hamiltonian is nontrivial in the $\hat{\phi}$ operators (through the $\hat{\phi}$ dependence of R), but quadratic in the f operators. In the following, we will thus carry out a mean-field approximation for the bosons and integrate out the f fields.

B. Mean-field approximation and matrix notation

We now condense the bosons; i.e., $\hat{\phi}_{Bn}$ is chosen to be a c number (and $\hat{\phi}_{Bn}^\dagger$ becomes ϕ_{Bn}^*). For notational convenience,

we define the $2^{\mathcal{N}_c} \times 2^{\mathcal{N}_c}$ matrices Φ and F :

$$[\Phi]_{An} \equiv \phi_{An}, \quad (17)$$

$$[F_\alpha]_{nm} \equiv f \langle n | f_\alpha | m \rangle_f. \quad (18)$$

In particular, $[\Phi^\dagger]_{nA} = [\Phi]_{An}^* = \phi_{An}^*$. We can always order the $|A\rangle$ states in such a way that $\langle A | c_\alpha | B \rangle = [F_\alpha]_{AB}$. In particular, $[F_\alpha^\dagger]_{AB} = [F_\alpha]_{BA}^* = (\langle B | c_\alpha | A \rangle)^* = \langle A | c_\alpha^\dagger | B \rangle$. If the coefficients of the F matrix are real (which is the case if one is dealing with Fock states, which is always possible), then

$$[F_\alpha^\dagger]_{AB} = [F_\alpha]_{BA}. \quad (19)$$

Thus, the expressions for the constraints become

$$\text{Tr}[\Phi \Phi^\dagger] = 1, \quad (20a)$$

$$f_\alpha^\dagger f_\beta = \Delta_{\alpha, \beta}^p \quad \forall \alpha, \beta. \quad (20b)$$

with

$$\begin{aligned} \Delta_{\alpha\beta}^p & \equiv \sum_{Anmp} f \langle m | f_\alpha^\dagger | p \rangle_f \langle p | f_\beta | n \rangle_f [\Phi^\dagger]_{nA} \Phi_{Am} \\ & = \text{Tr}[F_\alpha^\dagger F_\beta \Phi^\dagger \Phi]. \end{aligned} \quad (21)$$

Furthermore,

$$\begin{aligned} R_{\beta\alpha} & = \sum_\gamma \sum_{ABnm} F_{\alpha, A, B}^\dagger F_{\gamma, nm}^\dagger [\Phi^\dagger]_{nA} [\Phi]_{Bm} \\ & \quad \times [(\Delta^p(1 - \Delta^p))^{-1/2}]_{\gamma\beta} \\ & = \sum_\gamma \text{Tr}[\Phi^\dagger F_\alpha^\dagger \Phi F_\gamma] [(\Delta^p(1 - \Delta^p))^{-1/2}]_{\gamma\beta}, \end{aligned}$$

where, to obtain the second line, we have assumed F to be real valued [Eq. (19)]. Equivalently, we have

$$R_{\gamma\alpha} \{[\Delta^p(1 - \Delta^p)]^{1/2}\}_{\gamma\beta} = \text{Tr}[\Phi^\dagger F_\alpha^\dagger \Phi F_\beta]. \quad (22)$$

The local part of the Hamiltonian reads

$$\begin{aligned} \underline{H}_{\text{loc}} & = \sum_i \sum_{A_i B_i n_i} \langle A_i | H_{\text{loc}} | B_i \rangle [\Phi^\dagger]_{n_i A_i} \Phi_{B_i n_i} \\ & = \sum_i \text{Tr}[\Phi^\dagger H_{\text{loc}} \Phi]. \end{aligned} \quad (23)$$

C. Mean-field free-energy and Lagrange equations

The problem at hand now boils down to minimizing the free energy, a function of the slave-boson mean fields Φ_{An} , under the constraints (20a) and (20b). In the original formulation [19], inspired by previous slave boson approaches [30], the fulfillment of the constraints was enforced by introducing two Lagrange multipliers E^c and λ . It was then proposed [25,28,29], in order to overcome the remaining strong nonlinearity of the free energy as a function of Φ , to turn Eqs (21) and (22) into constraints, thereby making the free energy quadratic in Φ at the price of adding two more Lagrange multipliers λ^c and \mathcal{D} and turning Δ^p and R into independent variables. Following this strategy, the free energy

of the system is given by

$$\Omega[\Phi, R, \Delta^p; E^c, \lambda, \mathcal{D}, \lambda^c] \equiv -\beta \log \int \mathcal{D}[f^*, f] e^{-S[\Phi, R, \Delta^p; E^c, \lambda, \mathcal{D}, \lambda^c]}, \quad (24)$$

with

$$\begin{aligned} S[\Phi, R, \Delta^p; E^c, \lambda, \mathcal{D}, \lambda^c] = & - \sum_{ki\omega} \text{Tr} \log \{ i\omega - R_{\alpha\gamma} \bar{\varepsilon}_k^{\gamma\delta} R_{\delta\beta}^\dagger - \lambda_{\alpha\beta} + \mu \delta_{\alpha,\beta} \} e^{i\omega 0^+} \\ & + \sum_i \text{Tr} \left[E^c (\Phi^\dagger \Phi - 1) + \sum_{\alpha\beta} (\mathcal{D}_{\alpha\beta} \Phi^\dagger F_\alpha^\dagger \Phi F_\beta + \text{H.c.}) + \sum_{\alpha\beta} \lambda_{\alpha\beta}^c \Phi^\dagger \Phi F_\alpha^\dagger F_\beta + \Phi^\dagger H_{\text{loc}} \Phi \right] \\ & - \sum_{i:\alpha\beta} (\lambda_{\alpha\beta} + \lambda_{\alpha\beta}^c) \Delta_{\alpha\beta}^p - \sum_{i:\alpha\beta\gamma} (\mathcal{D}_{\alpha\beta} R_{\gamma\alpha} + \text{c.c.}) [\Delta^p (1 - \Delta^p)]_{\gamma\beta}^{1/2}. \end{aligned} \quad (25)$$

Here, \sum_i is shorthand for $\sum_i^{\mathcal{N}_i}$, and in principle, all the variables $\Phi, R, \Delta^p, E^c, \lambda, \mathcal{D}, \lambda^c$ depend on the site index i but we dropped it since we will be looking for uniform solutions.

The slave boson amplitudes Φ_{An} appear only in the second line. Inspired by the fact that these amplitudes are defined on a local Hilbert space (spanned by A) and its copy (spanned by n), one can introduce [28] the corresponding tensor-product space, spanned by the basis $\{|A\rangle \otimes |n\rangle_a\}_{A,n}$, where states $|A\rangle$ are created by impurity operators c^\dagger, c and $|n\rangle_a$ by ‘‘bath’’ operators a^\dagger, a . In this construction, one interprets the amplitudes Φ_{An} as coefficients of the Schmidt decomposition of general states $|\Phi\rangle$ of this product space:

$$|\Phi\rangle \equiv \sum_{An} e^{i\frac{\pi}{2} N_A (N_A - 1)} \Phi_{An} \hat{U}_{\text{ph}} |A\rangle |n\rangle_a, \quad (26)$$

where \hat{U}_{ph} is a particle-hole transformation acting only on the a operators. With this definition and the phase factor, one has [28]

$$\text{Tr}[F_\alpha^\dagger F_\beta \Phi^\dagger \Phi] = \langle \Phi | a_\beta a_\alpha^\dagger | \Phi \rangle, \quad (27a)$$

$$\text{Tr}[\Phi^\dagger F_\alpha^\dagger \Phi F_\beta] = \langle \Phi | c_\alpha^\dagger a_\beta | \Phi \rangle, \quad (27b)$$

which allows us to express the right-hand sides of Eqs (21) and (22) as correlators of the c and a operators. Besides, the second line of the right-hand side of (25) becomes $E^c (\langle \Phi | \Phi \rangle - 1) + \langle \Phi | \hat{H}_{\text{embed}} | \Phi \rangle$, with H_{embed} defined in Eq. (3). This Hamiltonian describes an Anderson impurity level, described by the fields c, c^\dagger interacting through the local Hamiltonian H_{int} , hybridized with noninteracting bath levels a, a^\dagger of energies $-\lambda^c$ via the hybridization strengths \mathcal{D} .

Finally, one extremizes the free energy with respect to its variables to find the Lagrange equations of the problem:

$$\Delta_{\alpha\beta}^p = \sum_{k \in \text{BZ}, i\omega} [i\omega - R \bar{\varepsilon}_k R^\dagger - \lambda + \mu]_{\beta\alpha}^{-1} e^{i\omega 0^+}, \quad (28a)$$

$$\sum_{\mu} \{ [\Delta^p (1 - \Delta^p)]^{1/2} \}_{\alpha\mu} \mathcal{D}_{\beta\mu} = \sum_{k \in \text{BZ}, i\omega} \{ [\bar{\varepsilon}_k R^\dagger] [i\omega - R \bar{\varepsilon}_k R^\dagger - \lambda + \mu]^{-1} \}_{\beta\alpha} e^{i\omega 0^+}, \quad (28b)$$

$$\lambda_{\alpha\beta}^c = -\lambda_{\alpha\beta} - \sum_{\gamma\delta\eta} \left\{ \mathcal{D}_{\gamma\delta} R_{\eta\gamma} \frac{\partial \{ [\Delta^p (1 - \Delta^p)]^{1/2} \}_{\eta\delta}}{\partial \Delta_{\alpha\beta}^p} + \text{c.c.} \right\}, \quad (28c)$$

$$\hat{H}_{\text{embed}} | \Phi \rangle = E^c | \Phi \rangle, \quad (28d)$$

$$\langle \Phi | a_\beta a_\alpha^\dagger | \Phi \rangle = \Delta_{\alpha\beta}^p, \quad (28e)$$

$$\langle \Phi | c_\alpha^\dagger a_\beta | \Phi \rangle = R_{\gamma\alpha} \{ [\Delta^p (1 - \Delta^p)]^{1/2} \}_{\gamma\beta}. \quad (28f)$$

D. Solution of the Lagrange equations

Root-solving. In previous works [25,28,29], the Lagrange equations were solved by formulating the problem as a root-solving procedure by defining the functions

$$\mathcal{F}^{(1)}[R, \lambda] \equiv \langle \Phi | a_\beta a_\alpha^\dagger | \Phi \rangle - \Delta_{\alpha\beta}^p, \quad (29a)$$

$$\mathcal{F}^{(2)}[R, \lambda] \equiv \langle \Phi | c_\alpha^\dagger a_\beta | \Phi \rangle - R_{\gamma\alpha} \{ [\Delta^p (1 - \Delta^p)]^{1/2} \}_{\gamma\beta}. \quad (29b)$$

$\mathcal{F}^{(1)}$ and $\mathcal{F}^{(2)}$ are implicit functions of R and λ : For a given R and λ , one can successively compute $\Delta^p, \mathcal{D}, \lambda^c$, and $|\Phi\rangle$ by using Eqs. (28a), (28b), (28c), and (28d), respectively. The fulfillment of the last two equations, Eqs. (28e) and (28f), thus amounts to solving the root problem:

$$\mathcal{F}^{(1)}[R, \lambda] = 0,$$

$$\mathcal{F}^{(2)}[R, \lambda] = 0.$$

We note that the same Lagrange equations can be cast as different root problems (depending on the choice of free variable; for instance, one could have chosen \mathcal{D} and λ^c instead of R and λ). In the next paragraph, we give an alternative route to solve the Lagrange equations to shed light on the relation of RISB with the DMFT method.

Forward recursion and comparison to DMFT. One can alternatively solve the Lagrange equations in a forward recursive fashion, as is usually done in DMFT:

- (1) Start from a guess R and λ .
- (2) Compute the local density matrix Δ^p using (28a) and the local “kinetic energy,”

$$[\mathcal{K}_{\text{loc}}]_{\alpha\beta} \equiv \sum_{k \in \text{BZ}, i\omega} [\{\tilde{\varepsilon}_k R^\dagger\} [i\omega - R\tilde{\varepsilon}_k R^\dagger - \lambda + \mu]^{-1}]_{\beta\alpha} e^{i\omega 0^+}. \quad (30)$$

- (3) Compute \mathcal{D} and λ^c using Eq. (28b), i.e.,

$$\mathcal{D}_{\beta\alpha} = \{[\Delta^p(1 - \Delta^p)]^{-1/2}\}_{\alpha\mu} [\mathcal{K}_{\text{loc}}]_{\mu\beta}, \quad (31)$$

and Eq. (28c).

- (4) Solve the embedded problem Eq. (28d) for its (normalized) ground state $|\Phi\rangle$.

- (5) Compute a new R as

$$R_{\gamma\alpha} = M_{\alpha\beta} \{[N^a(1 - N^a)]^{-1/2}\}_{\beta\gamma} \quad (32)$$

with

$$N_{\alpha\beta}^a \equiv \langle \Phi | a_\beta a_\alpha^\dagger | \Phi \rangle, \quad (33a)$$

$$M_{\alpha\beta} \equiv \langle \Phi | c_\alpha^\dagger a_\beta | \Phi \rangle, \quad (33b)$$

and a new λ as

$$\lambda_{\alpha\beta} = -\lambda_{\alpha\beta}^c - \sum_{\gamma\delta\eta} \left\{ \mathcal{D}_{\gamma\delta} R_{\eta\gamma} \frac{\partial \{[N^a(1 - N^a)]^{1/2}\}_{\eta\delta}}{\partial N_{\alpha\beta}^a} + \text{c.c.} \right\}. \quad (34)$$

- (6) Go back to step 2 until convergence of R and λ .

This cycle is illustrated in Fig. 2(b): In RISB, the impurity model is solved for $N_{\alpha\beta}$ and $M_{\alpha\beta}$ to obtain the *two* matrices $R_{\alpha\beta}$ and $\lambda_{\alpha\beta}$, which are used as a parametrization of the lattice self-energy:

$$\Sigma(\mathbf{k}, i\omega_n) \approx i\omega_n [\mathbf{1} - (R^\dagger R)^{-1}] + R^{-1} \lambda [R^\dagger]^{-1} - \varepsilon_{\text{loc}}. \quad (35)$$

The impurity model is also parametrized by *two* matrices, the hybridization strengths $\mathcal{D}_{\alpha\beta}$ and bath hopping parameters $\lambda_{\alpha\beta}^c$, which are adjusted in such a way that the local density matrix Δ^p coincides with N and $\{[\Delta^p(1 - \Delta^p)]^{1/2}\}^\dagger R$ coincides with M [Eqs. (28e)–(28f)].

In practice, this loop allows us to obtain stable solutions in the Mott phase of the Hubbard model more easily than by solving the Lagrange equations as a root problem.

By contrast, DMFT (whose self-consistent loop is illustrated in the top panel of Fig. 2) requires the *frequency-dependent* local Green’s function $G_{\text{loc}}(i\omega_n)$ [defined as the \mathbf{k} summation of the lattice Green’s function $G(\mathbf{k}, i\omega)$ defined in Eq. (5)] to match the impurity Green’s function $G_{\text{imp}}(i\omega_n)$ [Eq. (4)] by adjusting the hybridization function $\Delta(i\omega_n)$, at the cost of approximating the lattice self-energy by the impurity

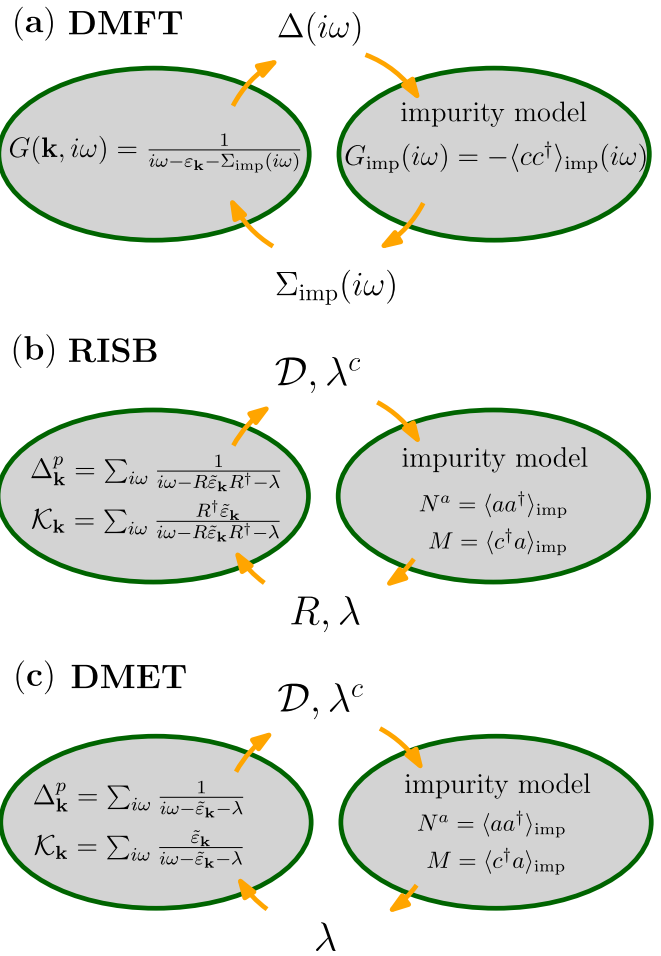


FIG. 2. From top to bottom: DMFT, RISB, and DMET: iterative solution by forward recursion. (The chemical potential is not indicated for conciseness.)

self-energy $\Sigma_{\text{imp}}(i\omega_n)$: All these functions depend on an infinite number of Matsubara frequencies, and correspondingly DMFT’s impurity model has an infinite number of bath levels: $\Delta(i\omega_n)$ can in general only be represented by an infinity of bath sites:

$$\Delta_{\alpha\beta}(i\omega_n) = \sum_{b=1}^{\infty} \sum_{\gamma\delta} \mathcal{D}_{\alpha\gamma}^b [i\omega \mathbf{1} + [\lambda^c]^b]_{\gamma\delta}^{-1} [\mathcal{D}_{\beta\delta}^b]^*, \quad (36)$$

contrary to RISB in which $b = 1$. Note that in the DMFT literature, \mathcal{D} (resp., λ^c) is usually denoted as V (resp., $-\epsilon$).

Thus, RISB can be viewed as a well-defined way of drastically truncating the number of bath levels in the impurity problem and of parametrizing the low-energy behavior of the impurity self-energy by two observables, the matrices R and λ . Beyond the reduced number of bath levels of the impurity model, RISB only necessitates the computation of *static* correlators, $\langle \Phi | a_\beta a_\alpha^\dagger | \Phi \rangle$ and $\langle \Phi | c_\alpha^\dagger a_\beta | \Phi \rangle$, whereas DMFT requires the full frequency dependence of the Green’s function $G_{\text{imp}}(i\omega_n)$.

Alternative approaches to truncate the number of bath levels exist: two-site DMFT [14] uses the low- and high-frequency limit of the DMFT self-consistency condition $G_{\text{imp}}(i\omega) = G_{\text{loc}}(i\omega)$ to fix the position and hybridization of a single

bath level (in the context of a single-band model; see also Refs. [48,49] for another prescription in a multiorbital context).

In a different perspective, solving the DMFT impurity model with an exact diagonalization method [50] also relies on a truncation procedure. There, the number as well as position and hybridization of bath sites is dictated not by formal considerations (as in RISB or two-site DMFT) but by computational limitations attached to the former and a (somewhat arbitrary) fitting procedure [using the parametrization of Eq. (36)] for the latter.

E. Equivalence to the multiband Gutzwiller approximation

RISB has been shown to be equivalent [31] to the multiband formulation of the Gutzwiller approximation. In other words, the above derivation can be carried out, instead of introducing slave bosons ϕ and quasiparticle fields f , by minimizing the variational energy $\langle \Psi_G | H | \Psi_G \rangle$ over the Gutzwiller wave functions

$$|\Psi_G(R, \lambda)\rangle \equiv \prod_i \mathcal{P}_i(R, \lambda) |\Psi_0(R, \lambda)\rangle, \quad (37)$$

where $|\Psi_0\rangle$ is a noninteracting wave function (a Slater determinant $|\Psi_0\rangle = \prod_{p=1}^{n_{\text{occ}}} c_p^\dagger |0\rangle$ with $p = 1 \dots n_{\text{occ}}$ denoting the occupied states) and \mathcal{P}_i is a projector on the local many-body Hilbert space defined above:

$$\mathcal{P}_i = \sum_{A,B} \Lambda_{A,B}(R, \lambda) |A_i\rangle \langle B_i| \quad (38)$$

(the connection between the Λ matrix and the slave boson matrix Φ_{An} is explored, e.g., in Ref. [25]).

This is done under the ‘‘Gutzwiller constraints’’

$$\forall i \quad \langle \Psi_0 | \mathcal{P}_i^\dagger \mathcal{P}_i | \Psi_0 \rangle = 1, \quad (39a)$$

$$\forall i, \alpha, \beta \quad \langle \Psi_0 | \mathcal{P}_i^\dagger \mathcal{P}_i c_{i\alpha}^\dagger c_{i\beta} | \Psi_0 \rangle = \langle \Psi_0 | c_{i\alpha}^\dagger c_{i\beta} | \Psi_0 \rangle. \quad (39b)$$

which can be shown (see, e.g., Ref. [31]) to be equivalent to the aforementioned RISB constraints, Eqs. (20a) and (20b).

In the next section, we show that the recently introduced DMET is a simplified form of RISB where R is approximated by the identity matrix.

III. DENSITY-MATRIX EMBEDDING THEORY: A SIMPLIFIED RISB

Density-matrix embedding theory (DMET) has been introduced as a simplified version of DMFT [20]. As outlined in Sec. I, DMET replaces the original lattice problem [Eq. (1)] with a reference problem [Eq. (2)] where the effect of correlations is described by a one-body potential λ (usually called u in the DMET literature). In other words, the self-energy is approximated by a static, local (within a cell) potential

$$\Sigma_{\alpha\beta}(\mathbf{k}, i\omega_n) \approx u_{\alpha\beta}. \quad (40)$$

Like in DMFT and RISB, the approximate form of the self-energy (here a matrix, u) is obtained in a nontrivial way by a self-consistent mapping of the reference problem onto an embedded local problem with fewer correlated degrees of freedom. The parameters of this impurity problem are then adjusted (through an adjustment of u) to match the

(one-particle) density matrix of the embedded problem with the projection of the density matrix of the reference problem onto the embedded subspace.

In wave-function language, DMET corresponds to making the following variational ansatz for the ground-state wave function:

$$|\Psi_{\text{DMET}}\rangle \equiv |\Psi_0(u)\rangle, \quad (41)$$

where $|\Psi_0\rangle$ is a Slater determinant and u is obtained by matching the density matrices as discussed above.

Several equivalent derivations of DMET have been given in the literature [20,21,32–36,51]. Here, we give a derivation similar to Ref. [34] but at times use different notation or terminology to make the connection to the RISB or Gutzwiller formalism more transparent.

A. Summary of the DMET self-consistency

In this subsection, we give a brief summary of the DMET workflow. Having mapped the lattice problem onto a reference problem consisting in an interacting *fragment* (of size \mathcal{N}_c) and a noninteracting *environment* (as illustrated in Fig. 1), DMET defines an embedded subspace through a projection operator P which projects the $\mathcal{N}_c + (\mathcal{N} - \mathcal{N}_c)$ degrees of freedom of the fragment + environment onto the $\mathcal{N}_c + \mathcal{N}_c$ degrees of freedom of the embedded (i.e., impurity + bath) problem. Then, the DMET self-consistency consists in matching

(i) the density matrix of the embedded problem

$$\rho_{\text{imp}} \equiv \begin{bmatrix} \langle \Phi | c_\alpha^\dagger c_\beta | \Phi \rangle & \langle \Phi | c_\alpha^\dagger a_\beta | \Phi \rangle \\ \langle \Phi | a_\alpha^\dagger c_\beta | \Phi \rangle & \langle \Phi | a_\alpha^\dagger a_\beta | \Phi \rangle \end{bmatrix}, \quad (42)$$

where $|\Phi\rangle$ is the ground state of H_{embed} [Eq. (3)], itself related to H_{eff} [Eq. (2)] by ‘‘projection’’ by P , namely

$$H_{\text{embed}} = \hat{H}_{\text{loc}}[\{c_\alpha^\dagger, c_\alpha\}] + \sum_{\alpha\beta} \begin{bmatrix} c_\alpha \\ a_\alpha \end{bmatrix}^\dagger [h_{\text{embed}}]_{\alpha\beta} \begin{bmatrix} c_\beta \\ a_\beta \end{bmatrix}, \quad (43)$$

with

$$h_{\text{embed}} \equiv P^\dagger h P, \quad (44)$$

and h the one-body part of H_{eff} ,

$$h \equiv t + \begin{bmatrix} 0 & & 0 \\ & u & \\ 0 & & \ddots \\ & & & u \end{bmatrix} \quad (45)$$

[the u block is of size $(\mathcal{N} - \mathcal{N}_c) \times (\mathcal{N} - \mathcal{N}_c)$], with

(ii) the projection of the density matrix ρ of the reference problem in the embedded subspace,

$$\rho_{\text{embed}} \equiv P^\dagger \rho P, \quad (46)$$

with

$$\rho_{i\alpha, j\beta} = \sum_{i\omega} e^{i\omega 0^+} [i\omega \mathbf{1} - h_{\text{TI}} + \mu]_{i\alpha, j\beta}^{-1}. \quad (47)$$

We recall that the Latin indices i, j label the unit cells, while the Greek indices $\alpha, \beta = 1 \dots \mathcal{N}_c$ label the internal orbital and cluster degrees of freedom. In the above expression, h_{TI} is the

translation-invariant version of h ; i.e., it contains a potential u on the upper-left ($i = 0, j = 0$) block: $[h_{\text{TI}}]_{i\alpha, j\beta} = h_{i\alpha, j\beta} + u_{\alpha\beta} \delta_{i,0} \delta_{j,0}$. In practice, we will see that exactly *matching* those two density matrices is in general impossible, so that a *minimization* of a distance between both matrices is carried out.

In the following subsection, we show how the projector P is constructed.

B. Construction of the impurity and bath operators

In this section, we define the mapping from the effective medium (with \mathcal{N} orbitals) to the embedded problem (with $2\mathcal{N}_c$ orbitals), or in other words we construct the projector P .

We start by explaining how to transform from the fragment (size \mathcal{N}_c) to the impurity (size \mathcal{N}_c) orbitals. First off, diagonalizing the lattice density matrix ρ [given in Eq. (47)] yields a transformation $D_{\text{F}}^{\text{occ}}$ from the single-site levels of the fragment (denoted by Greek indices) to the occupied levels of H_{eff} (see Appendix A for details).

Second, we need to find a transformation from the occupied levels to the impurity orbitals. The central object for doing so is the overlap matrix between the fragment and the occupied states of the lattice, defined as

$$S_{pq}^{\text{occ}} \equiv \langle \phi_p | P^{\text{F}} | \phi_q \rangle, \quad (48)$$

with p and q labeling two occupied states of H_{eff} ($1 \leq p, q \leq n_{\text{occ}}$), ϕ_p being the corresponding single-particle state, $|\phi_p\rangle \equiv c_p^\dagger |0\rangle$, and P^{F} the projector on the fragment ($P^{\text{F}} \equiv \sum_{\alpha=1}^{\mathcal{N}_c} |\phi_\alpha\rangle \langle \phi_\alpha|$). We show in Appendix A that this matrix can be transformed to a diagonal form,

$$S^{\text{occ}} = V_{\text{F}} n^0 V_{\text{F}}^\dagger, \quad (49)$$

where n^0 is a $\mathcal{N}_c \times \mathcal{N}_c$ diagonal matrix, and V_{F} is a $n_{\text{occ}} \times \mathcal{N}_c$ rectangular matrix such that $V_{\text{F}}^\dagger V_{\text{F}} = 1$. $[V_{\text{F}}]_{p, \alpha'}$ defines a transformation from the occupied states (p, \dots) to new states (denoted by primed Greek indices α', \dots) that correspond to the ‘‘natural orbitals’’ used, e.g., in Ref. [25].

With these two transformations, one defines the transformation from the fragment to the impurity as

$$\tilde{C}_{\text{F}} = D_{\text{F}}^{\text{occ}} V_{\text{F}},$$

or rather, with orthonormalized columns,

$$[C_{\text{F}}]_{\alpha\alpha'} \equiv \frac{[D_{\text{F}}^{\text{occ}}]_{\alpha p} [V_{\text{F}}]_{p\alpha'}}{\sqrt{n_{\alpha'}^0}}. \quad (50)$$

(To determine the normalization, we have used $\tilde{C}_{\text{F}}^\dagger \tilde{C}_{\text{F}} = V_{\text{F}}^\dagger D_{\text{F}}^{\text{occ}, \dagger} D_{\text{F}}^{\text{occ}} V_{\text{F}} = V_{\text{F}}^\dagger V_{\text{F}} n^0 V_{\text{F}}^\dagger V_{\text{F}} = n^0$.)

Likewise, the matrix which projects from the environment to the bath is defined as the product of the transformation from the environment levels to the occupied states (a matrix called $D_{\text{E}}^{\text{occ}}$) with the transformation from the occupied levels to the natural orbitals (V_{F}). After orthonormalization of the columns, we obtain

$$C_{\text{B}} \equiv \frac{D_{\text{E}}^{\text{occ}} V_{\text{F}}}{\sqrt{1 - n^0}}. \quad (51)$$

We thus define the projector,

$$\bar{P} \equiv \begin{bmatrix} C_{\text{F}} & \\ & C_{\text{B}} \end{bmatrix}, \quad (52)$$

which projects the lattice problem (fragment $\{c_{i\alpha}^\dagger\}_{1 \leq \alpha \leq \mathcal{N}_c}$ + environment $\{c_{i\alpha}^\dagger\}_{1 \leq i \leq \mathcal{N}/\mathcal{N}_c, 1 \leq \alpha \leq \mathcal{N}_c}$) onto the embedded problem (impurity $\{\tilde{c}_{\alpha'}^\dagger\}_{1 \leq \alpha' \leq \mathcal{N}_c}$ + bath $\{\tilde{a}_{\alpha'}^\dagger\}_{1 \leq \alpha' \leq \mathcal{N}_c}$):

$$\tilde{c}_{\alpha'}^\dagger = \sum_{\alpha=1}^{\mathcal{N}_c} c_{1\alpha}^\dagger [C_{\text{F}}]_{\alpha\alpha'}, \quad (53)$$

$$\tilde{a}_{\alpha'}^\dagger = \sum_{i=2}^{\mathcal{N}/\mathcal{N}_c} \sum_{\alpha=1}^{\mathcal{N}_c} c_{i\alpha}^\dagger [C_{\text{B}}]_{i\alpha;\alpha'}. \quad (54)$$

Instead of the natural-orbital basis, one can choose instead to use the original basis (denoted by unprimed Greek indices) as a single-site basis to express the creation operators c^\dagger and a^\dagger of the embedded problem. This is done by defining the alternative projector,

$$P \equiv \begin{bmatrix} \mathbf{1} & \\ & C_{\text{B}} C_{\text{F}}^\dagger \end{bmatrix}, \quad (55)$$

which is related to \bar{P} by a unitary transform,

$$P = \bar{P} \begin{bmatrix} C_{\text{F}}^\dagger & \\ & C_{\text{F}}^\dagger \end{bmatrix},$$

where \bar{P} projects into the natural orbitals and P projects into the original orbitals.

We note that the above construction corresponds to carrying out the Schmidt decomposition of $|\Psi_0(u)\rangle$ [20].

In the next subsection, we use P to project lattice observables onto the embedded subspace.

C. Projections in the embedded subspace

After constructing the impurity and bath levels, one can now map the density matrix and lattice Hamiltonian onto the embedded subspace.

1. Embedded density matrix

The projection of the density matrix onto the embedded subspace is defined in Eq. (46), and similarly for $\bar{\rho}_{\text{embed}}$. After a few algebraic steps detailed in Appendix B 1, we obtain

$$\bar{\rho}_{\text{embed}} \equiv \bar{P}^\dagger \rho \bar{P} = \begin{bmatrix} n^0 & \sqrt{n^0(1-n^0)} \\ \sqrt{n^0(1-n^0)} & 1-n^0 \end{bmatrix}, \quad (56)$$

i.e., $\bar{\rho}_{\text{embed}}$ is entirely determined by the occupations of the natural orbitals n^0 . Similarly, its expression in the original basis is

$$\rho_{\text{embed}} = \begin{bmatrix} \Delta^p & \sqrt{\Delta^p(1-\Delta^p)} \\ \sqrt{\Delta^p(1-\Delta^p)} & 1-\Delta^p \end{bmatrix}, \quad (57)$$

with

$$\Delta^p \equiv C_{\text{F}} n^0 C_{\text{F}}^\dagger = D_{\text{F}}^{\text{occ}} D_{\text{F}}^{\text{occ}, \dagger} = \rho_{\text{F}},$$

with ρ_{F} the top left $\mathcal{N}_c \times \mathcal{N}_c$ block of ρ . Thus, Δ^p (as defined in the RISB section) is the one-particle density matrix of the

fragment, ρ_F . Using (47), we thus have

$$\begin{aligned}\Delta_{\alpha\beta}^p &= \sum_{i\omega} e^{i\omega 0^+} [i\omega \mathbf{1} - t - u + \mu]_{1\alpha,1\beta}^{-1} \\ &= \sum_{k,i\omega} e^{i\omega 0^+} [i\omega \mathbf{1} - \varepsilon_k - u + \mu]_{\alpha,\beta}^{-1}.\end{aligned}$$

We define

$$\tilde{u}_{\alpha\beta} \equiv u_{\alpha\beta} + [\varepsilon_{\text{loc}}]_{\alpha\beta} \quad (58)$$

to obtain the analog of Eq. (28a) in the RISB formalism:

$$\Delta_{\alpha\beta}^p = \sum_{k,i\omega} e^{i\omega 0^+} [i\omega \mathbf{1} - \tilde{\varepsilon}_k - \tilde{u} + \mu]_{\alpha,\beta}^{-1}. \quad (59)$$

Equations (28a) and (59) can be identified provided

$$R = \mathbf{1}, \quad (60a)$$

$$\lambda = \tilde{u}. \quad (60b)$$

In the next subsection, we show that this identification holds for all other DMET observables.

2. Parameters of the embedded problem

Based on the two definitions of H_{embed} , Eqs. (3) and (43), we can write¹

$$h_{\text{embed}} = \begin{bmatrix} t_F & \mathcal{D} \\ \mathcal{D}^\dagger & -\lambda^c \end{bmatrix}. \quad (61)$$

Identifying the right-hand sides of Eqs. (44) and (61), and thanks to the definition [Eq. (55)] of P , one can show, after a few algebraic steps detailed in Appendix B 2, that

$$\mathcal{D} = \sum_{ki\omega} \tilde{\varepsilon}_k [i\omega - \tilde{\varepsilon}_k - \tilde{u}]^{-1} [\sqrt{\Delta^p(1 - \Delta^p)}]^{-1} \quad (62a)$$

and

$$\begin{aligned}\lambda^c &= -\tilde{u} - [\sqrt{(1 - \Delta^p)\Delta^p}]^{-1} \frac{\mathcal{K}_{\text{loc}}(1 - 2\Delta^p) + (1 - 2\Delta^p)\mathcal{K}_{\text{loc}}}{2} \\ &\quad \times [\sqrt{\Delta^p(1 - \Delta^p)}]^{-1},\end{aligned} \quad (62b)$$

which respectively correspond to Eqs. (28b) and (28c) with the identification (60a) and (60b).

D. Self-consistency conditions

As mentioned in a previous section, the DMET self-consistency conditions consist in matching the embedded density matrix ρ_{embed} obtained by projection of the lattice-density matrix onto the embedded subspace with the density matrix of the embedded or impurity problem, whose block structure reads

$$\rho_{\text{imp}} = \begin{bmatrix} N^c & M \\ M^\dagger & N^a \end{bmatrix}, \quad (63)$$

with N^a and M defined in Eqs. (33a) and (33b) and

$$N_{\alpha\beta}^c \equiv \langle \Phi | c_\alpha^\dagger c_\beta | \Phi \rangle, \quad (64)$$

where $|\Phi\rangle$ is the ground state of the impurity Hamiltonian, i.e., the solution of Eq. (28d). Thus, the self-consistency conditions explicitly read

$$\langle \Phi | a_\beta a_\alpha^\dagger | \Phi \rangle = \Delta_{\alpha\beta}^p, \quad (65a)$$

$$\langle \Phi | c_\alpha^\dagger a_\beta | \Phi \rangle = [\sqrt{\Delta^p(1 - \Delta^p)}]_{\alpha\beta}, \quad (65b)$$

$$\langle \Phi | c_\alpha^\dagger c_\beta | \Phi \rangle = \Delta_{\alpha\beta}^p. \quad (65c)$$

The first two lines, with the identification (60a), correspond to the RISB conditions (28e) and (28f).

E. Solution of the DMET equations: Overdetermination, idempotency, and alternative self-consistency conditions

The DMET equations presented in the previous sections have so far been solved in a forward recursive way:

- (1) Start from a guess for u .
- (2) Compute \mathcal{D} and λ^c from Δ^p and \mathcal{K}_{loc} .
- (3) Solve the impurity model for ρ_{imp} , i.e., for N^a , N^c , and M .

(4) From u , compute $\rho_{\text{embed}}(u)$ as given by Eq. (57). If $\rho_{\text{embed}}(u) = \rho_{\text{imp}}(u)$, self-consistency is reached and the solution is u . Otherwise, find u' such that $\rho_{\text{embed}}(u') = \rho_{\text{imp}}(u)$ and go back to step 2 with the new u' until self-consistency is reached.

This loop is different from the loop presented in Sec. II D. The potential advantage of this alternative forward recursion is that it in principle requires fewer computations of the impurity solution: the root problem,

$$\mathcal{F}_u(u') \equiv \rho_{\text{embed}}(u') - \rho_{\text{imp}}(u) = 0, \quad (66)$$

requires only one impurity computation [to compute $\rho_{\text{imp}}(u)$]. However, this root problem must be solved several times, so that the numerical gain is *a priori* unclear.

On the other hand, the DMET self-consistency condition leads to an overdetermined root problem: There is only one unknown u to satisfy three self-consistency conditions, Eqs. (65a), (65b), and (65c). In comparison, the root problem to be solved in RISB has as many unknowns (R and λ) as equations ($\mathcal{F}^{(1)} = 0$ and $\mathcal{F}^{(2)} = 0$). Another independent issue is that ρ_{embed} as given in Eq. (56) or (57) is idempotent (one can check that $\rho_{\text{embed}}^2 = \rho_{\text{embed}}$), with the consequence that its eigenvalues must be zero or one. That ρ_{imp} generically shares this property is improbable; in fact, converged RISB results in the literature (with $R \neq 1$) prove that ρ_{imp} is in general not idempotent.

This has led to the exploration of several (arbitrary) procedures in the literature: The original papers proposed to minimize the sum of the squared differences between the matrix elements of ρ_{embed} and ρ_{imp} [instead of trying to find the root of Eq. (66)]; other authors suggest to fulfill only the condition on the density [e.g., Eq. (65a)], a scheme dubbed “density embedding theory”, DET [34].

In Fig. 2 (bottom panel), we illustrate another possible recursive scheme to solve the DMET equations inspired from DMFT (this scheme corresponds to the forward recursion

¹The minus sign in front of λ^c stems from the fact that H_{embed} contains a term $\lambda^c a a^\dagger$ instead of the more familiar $\lambda^c a^\dagger a$.

presented in Sec. II D, only with $R = 1$). This figure, while emphasizing the similarities between the three methods, also hints at the overdetermination problem we just discussed: While in RISB, two observables are needed to compute (N^a and M) and parametrize (λ and R) the self-energy and to characterize the embedded problem (λ^c and \mathcal{D}), in DMET, two observables (N^a and M) are computed at the level of the embedded problem (and needed to describe it, λ^c and \mathcal{D}), but the self-energy is described by only one parameter (λ or u), possibly pointing to an underexploitation of the physical information contained in the solution of the impurity model.

IV. CONCLUSION

In this work, we have derived the relation between two methods, RISB and DMET, which can both be regarded as simplified versions of DMFT. As such, they can access regimes of parameters and systems for which the exact solution, via quantum Monte Carlo, of the DMFT impurity problem, is prohibitively costly if not out of reach due to the negative-sign problem or very large computing times.

We have shown that the DMET equations can be obtained from the RISB equations by setting the quasiparticle weight factor to 1 in RISB. This establishes a clear connection between these two methods, which are both based on the mapping of a strongly correlated problem onto a simplified problem describing correlated orbitals embedded in a noninteracting host.

An additional comparison among the methods is possible if one uses the interpretation of the RISB method as a linear expansion of a self-energy [28]. Therefore, if one focuses on the the low-energy behavior of the self-energy, DMFT has real and imaginary parts with a general frequency dependence, RISB keeps the constant and linear term in a real self-energy, and DMET is purely static. In this context, it is worth mentioning other approximate methods which use a very different parametrization of the self-energy in terms of a continuous fraction expansion (see, for instance, Refs. [52,53]).

This common perspective on the three methods naturally suggests transposing extensions of one method to the others. For instance, a simple generalization of the RISB and Gutzwiller ground-state energy to a temperature-dependent free energy, briefly exposed in Appendix C, can be used to derive a temperature-dependent DMET free energy.

This work opens additional questions for cluster extensions. For instance, DMET yields good spectra for the Hubbard model [39]. Given that RISB and DMET have the same computational cost (that of solving an impurity model with the same number of bath and impurity levels), similar calculations should be carried out with the RISB method to explore how that embedding accelerates the convergence to the thermodynamic limit for spectral properties.

Applications of DMFT to molecular systems already exist [54,55], but it has been difficult to extend it to complex molecules. On the other hand, DMET has been very successful in its applications to quantum chemistry [35]. It would be interesting to explore potential applications of RISB in that field as well.

ACKNOWLEDGMENT

This project is supported by the Department of Energy under Grant No. DE-FG02-99ER45761.

APPENDIX A: TRANSFORMATION OF THE OVERLAP MATRIX TO DIAGONAL FORM

We start by diagonalizing the noninteracting Hamiltonian h ; we obtain

$$h = D\epsilon D^\dagger,$$

with D being a $\mathcal{N} \times \mathcal{N}$ unitary matrix and $\epsilon = \text{diag}(\{\epsilon_k\}_{k=1\dots\mathcal{N}})$ a diagonal matrix. Thanks to the expression (47), D also diagonalizes the density matrix, i.e.,

$$\rho = DnD^\dagger, \quad (\text{A1})$$

with n a diagonal matrix with entries $n_{\mathbf{F}}(\epsilon_k)$. The first n_{occ} eigenvalues of ρ (i.e., the first n_{occ} entries of n) are unity (they correspond to the occupied states), while the other eigenvalues vanish (they correspond to the empty states).

We now split D into its fragment and its environment blocks:

$$D = \begin{bmatrix} D_{\text{F}} \\ D_{\text{E}} \end{bmatrix}, \quad (\text{A2})$$

where D_{F} is of size $\mathcal{N}_c \times \mathcal{N}$. Since D is unitary, the following properties hold:

$$\begin{aligned} D_{\text{F}}^\dagger D_{\text{F}} + D_{\text{E}}^\dagger D_{\text{E}} &= 1, \\ D_{\text{F}} D_{\text{F}}^\dagger &= 1, \\ D_{\text{E}} D_{\text{E}}^\dagger &= 1. \end{aligned} \quad (\text{A3})$$

We further decompose D_{F} into two blocks:

$$D_{\text{F}} = \begin{bmatrix} D_{\text{F}}^{\text{occ}} & D_{\text{F}}^{\text{unocc}} \end{bmatrix}, \quad (\text{A4})$$

with $D_{\text{F}}^{\text{occ}}$ being a $\mathcal{N}_c \times n_{\text{occ}}$ matrix. Note that (A3) implies

$$D_{\text{F}}^{\text{occ}\dagger} D_{\text{F}}^{\text{occ}} + D_{\text{E}}^{\text{occ}\dagger} D_{\text{E}}^{\text{occ}} = 1. \quad (\text{A5})$$

We now perform a singular value decomposition of $D_{\text{F}}^{\text{occ}}$. We obtain

$$D_{\text{F}}^{\text{occ}} = U \{\text{diag}\{\sqrt{n^0}, 0\}\} V^\dagger, \quad (\text{A6})$$

with U being a $\mathcal{N}_c \times \mathcal{N}_c$ unitary matrix, $\{\text{diag}\{\sqrt{n^0}, 0\}\}$ a $\mathcal{N}_c \times n_{\text{occ}}$ matrix (with $\text{diag}\{\sqrt{n^0}\}$ a $\mathcal{N}_c \times \mathcal{N}_c$ diagonal matrix, simply denoted as $\sqrt{n^0}$ in the following), and V a $n_{\text{occ}} \times n_{\text{occ}}$ unitary matrix. We decompose V into two blocks:

$$V = \begin{bmatrix} V_{\text{F}} & V_{\text{E}} \end{bmatrix}, \quad (\text{A7})$$

with V_{F} being a $n_{\text{occ}} \times \mathcal{N}_c$ matrix. The unitarity of V implies the properties

$$\begin{aligned} V_{\text{F}} V_{\text{F}}^\dagger + V_{\text{E}} V_{\text{E}}^\dagger &= 1, \\ V_{\text{F}}^\dagger V_{\text{F}} &= 1, \\ V_{\text{E}}^\dagger V_{\text{E}} &= 1. \end{aligned} \quad (\text{A8})$$

Plugging (A7) into (A6), we obtain

$$D_{\text{F}}^{\text{occ}} = U \sqrt{n^0} V_{\text{F}}^\dagger. \quad (\text{A9})$$

The last step is to notice that the overlap matrix S^{occ} , defined in Eq. (48), is also given by the expression

$$S^{\text{occ}} = D_F^{\text{occ},\dagger} D_E^{\text{occ}}. \quad (\text{A10})$$

Thus, using (A9), we obtain Eq. (49).

APPENDIX B: PROJECTIONS INTO THE EMBEDDED SUBSPACE

We start by noting that the transformation between site indices and natural orbital indices is given by C_F [defined in Eq. (50)], itself equal to U ,

$$C_F = \frac{U\sqrt{n^0}V_F^\dagger V_F}{\sqrt{n^0}} = U, \quad (\text{B1})$$

where we have used Eqs. (A9) and (A8).

1. Density matrix

Using the block decomposition of the lattice density matrix,

$$\rho = \begin{bmatrix} \rho_F & \rho_c \\ \rho_c^\dagger & \rho_E \end{bmatrix} \quad (\text{B2})$$

(with ρ_F a $\mathcal{N}_c \times \mathcal{N}_c$ matrix, and so on) and the expressions (A1), (A2), and (A4), we obtain

$$\rho = \begin{bmatrix} D_F^{\text{occ}} D_F^{\text{occ},\dagger} & D_F^{\text{occ}} D_E^{\text{occ},\dagger} \\ D_E^{\text{occ}} D_F^{\text{occ},\dagger} & D_E^{\text{occ}} D_E^{\text{occ},\dagger} \end{bmatrix}.$$

Thus, using Eq. (46),

$$\begin{aligned} \bar{\rho}^{\text{embed}} &= \begin{bmatrix} C_F^\dagger D_F^{\text{occ}} D_F^{\text{occ},\dagger} C_F, & C_F^\dagger D_F^{\text{occ}} D_E^{\text{occ},\dagger} C_B \\ C_B^\dagger D_E^{\text{occ}} D_F^{\text{occ},\dagger} C_F, & C_B^\dagger D_E^{\text{occ}} D_E^{\text{occ},\dagger} C_B \end{bmatrix} \\ &= \begin{bmatrix} \frac{V_F^\dagger D_F^{\text{occ},\dagger} D_F^{\text{occ}} D_F^{\text{occ},\dagger} V_F}{\sqrt{n^0}}, & \frac{V_F^\dagger D_F^{\text{occ},\dagger} D_E^{\text{occ}} D_E^{\text{occ},\dagger} V_F}{\sqrt{n^0}} \\ \frac{V_F^\dagger D_E^{\text{occ},\dagger} D_F^{\text{occ}} D_F^{\text{occ},\dagger} V_F}{\sqrt{1-n^0}}, & \frac{V_F^\dagger D_E^{\text{occ},\dagger} D_E^{\text{occ}} D_E^{\text{occ},\dagger} V_F}{\sqrt{1-n^0}} \end{bmatrix} \\ &= \begin{bmatrix} n^0 & \sqrt{n^0(1-n^0)} \\ \sqrt{n^0(1-n^0)} & 1-n^0 \end{bmatrix}. \end{aligned} \quad (\text{B3})$$

2. Parameters of the embedded Hamiltonian

Identifying the blocks of Eqs (44) and (61), and using Eq (55), we obtain

$$\mathcal{D} = h_c C_B C_F^\dagger = D_F \epsilon D_E^\dagger \frac{D_E^{\text{occ}} V_F}{\sqrt{1-n^0}} \frac{V_F^\dagger D_F^{\text{occ},\dagger}}{\sqrt{n^0}}, \quad (\text{B4})$$

$$\begin{aligned} \lambda^c &= -C_F C_B^\dagger h_E C_B C_F^\dagger, \\ &= -\frac{D_F^{\text{occ}} V_F}{\sqrt{n^0}} \frac{V_F^\dagger D_E^{\text{occ},\dagger}}{\sqrt{1-n^0}} D_E \epsilon D_E^\dagger \frac{D_E^{\text{occ}} V_F}{\sqrt{1-n^0}} \frac{V_F^\dagger D_F^{\text{occ},\dagger}}{\sqrt{n^0}}. \end{aligned} \quad (\text{B5})$$

Let us simplify \mathcal{D} :

$$\begin{aligned} \mathcal{D} &= D_F \epsilon D_E^\dagger D_E^{\text{occ}} V_F U^\dagger [\sqrt{(1-\Delta^p)\Delta^p}]^{-1} U V_F^\dagger V_F \sqrt{n^0} U^\dagger \\ &= D_F \epsilon D_E^\dagger D_E^{\text{occ}} D_F^{\text{occ},\dagger} U [\sqrt{n^0}]^{-1} U^\dagger [\sqrt{(1-\Delta^p)}]^{-1} \\ &= h_c \rho_c^\dagger [\sqrt{\Delta^p(1-\Delta^p)}]^{-1}. \end{aligned} \quad (\text{B6})$$

Besides,

$$\begin{aligned} [h_c \rho_c^\dagger]_{\alpha\beta} &= \sum_{j\gamma} [t_c]_{\alpha,j\gamma} [\rho_c^\dagger]_{j\gamma,\beta} \\ &= \sum_{j\gamma} [\tilde{t}]_{1\alpha,j\gamma} [\rho]_{j\gamma,1\beta} \\ &= \sum_{k,k',\gamma} \sum_j e^{i(k-k')\cdot R_j} [\tilde{\epsilon}(\mathbf{k})]_{\alpha,\gamma} [\rho(\mathbf{k}')]_{\gamma,\beta} \\ &= \sum_{k,\gamma} [\tilde{\epsilon}(\mathbf{k})]_{\alpha,\gamma} [\rho(\mathbf{k})]_{\gamma,\beta} \\ &= \sum_{k,\gamma} [\tilde{\epsilon}(\mathbf{k})]_{\alpha,\gamma} \sum_{i\omega} e^{i\omega 0^+} [i\omega \mathbf{1} - \tilde{\epsilon}(\mathbf{k}) - \tilde{u}]_{\gamma,\beta}^{-1}. \end{aligned}$$

In the first line, we have used the block structure (45). The second line follows from the definition of t_c and \tilde{t} , the third line from the definition of the Fourier transform, Eq. (7), and the fifth line from Eq. (47). This yields Eq. (62a) of the main text.

Comparing with Eq. (30), we note that

$$h_c \rho_c^\dagger = \mathcal{K}_{\text{loc}} [R = \mathbf{1}, \lambda = \tilde{u}]. \quad (\text{B7})$$

Let us now simplify λ^c :

$$\begin{aligned} \lambda^c &= -U\sqrt{n^0}V_F^\dagger V_F U^\dagger [\sqrt{\Delta^p(1-\Delta^p)\Delta^p}]^{-1} U V_F^\dagger D_E^{\text{occ},\dagger} \\ &\quad \times D_E \epsilon D_E^\dagger D_E^{\text{occ}} V_F U^\dagger [\sqrt{(1-\Delta^p)\Delta^p}]^{-1} U V_F^\dagger V_F \sqrt{n^0} U^\dagger \\ &= -[\sqrt{(1-\Delta^p)}]^{-1} U [\sqrt{n^0}]^{-1} U^\dagger D_F^{\text{occ}} D_E^{\text{occ},\dagger} \\ &\quad \times D_E \epsilon D_E^\dagger D_E^{\text{occ}} D_F^{\text{occ},\dagger} U [\sqrt{n^0}]^{-1} U^\dagger [\sqrt{(1-\Delta^p)}]^{-1} \\ &= -[\sqrt{(1-\Delta^p)\Delta^p}]^{-1} \rho_c h_E \rho_c^\dagger [\sqrt{\Delta^p(1-\Delta^p)}]^{-1}. \end{aligned}$$

To simplify $\rho_c h_E \rho_c^\dagger$, let us first notice

$$\begin{aligned} \mathcal{K}_{\text{loc}} &= h_c \rho_c^\dagger = D_F \epsilon D_E^\dagger D_E n D_F^\dagger \\ &= D_F \epsilon n D_F^\dagger - D_F \epsilon D_F^\dagger D_F n D_F^\dagger \\ &= D_F \epsilon n D_F^\dagger - h_F \Delta^p. \end{aligned}$$

Hence,

$$\begin{aligned} \rho_c h_E \rho_c^\dagger &= D_F n D_E^\dagger D_E \epsilon D_E^\dagger D_E n D_F^\dagger \\ &= D_F n \epsilon n D_F^\dagger + D_F n D_F^\dagger D_F \epsilon D_F^\dagger D_F n D_F^\dagger \\ &\quad - D_F n \epsilon D_F^\dagger D_F n D_F^\dagger - D_F n D_F^\dagger D_F \epsilon n D_F^\dagger \\ &= \mathcal{K}_{\text{loc}} + h_F \Delta^p + \Delta^p h_F \Delta^p \\ &\quad - (\mathcal{K}_{\text{loc}} + h_F \Delta^p) \Delta^p - \Delta^p (\mathcal{K}_{\text{loc}} + h_F \Delta^p) \\ &= \frac{1}{2} [\mathcal{K}_{\text{loc}} (1 - 2\Delta^p) + (1 - 2\Delta^p) \mathcal{K}_{\text{loc}}] \\ &\quad + \Delta^p (1 - \Delta^p) h_F. \end{aligned}$$

This yields Eq. (62b) of the main text.

APPENDIX C: GROUND-STATE ENERGY AND FINITE-TEMPERATURE EXTENSION

At $T = 0$, the total energy in RISB is given by

$$E = \sum_k \text{Tr}[n_F(R\tilde{\epsilon}_k R^\dagger + \lambda - \mu)(R\tilde{\epsilon}_k R^\dagger)] + \sum_i \text{Tr}[H_{\text{loc}}\Phi_i\Phi_i^\dagger], \quad (\text{C1})$$

where n_F is the Fermi function and H_{loc} contains the chemical potential μ .

Note that it is straightforward to show that, using Eqs. (28b), (28f), and (27b), and with $R = 1$, Eq. (C1) is equivalent to the DMET ground-state energy given in [20,33]

$$E = \sum_i \left\{ \text{Tr} \sum_{\alpha\beta} (\mathcal{D}_{\alpha\beta} \Phi_i^\dagger F_\alpha^\dagger \Phi_i F_\beta) + \text{Tr}[H_{\text{loc}}\Phi_i\Phi_i^\dagger] \right\}. \quad (\text{C2})$$

In RISB, Eqs. (C1) and (C2) produce the same total energies because the Lagrange equations, Eqs. (28a)–(28f), are exactly satisfied. However, in DMET, since the Lagrange equation, Eq. (66), can merely be minimized, Eqs. (C1) and (C2) no

longer yield the same energy. One has to evaluate the total energy using Eq. (C2) as done in the DMET literature.

The RISB formalism can be readily extended to finite temperatures, as will be explored in a separate publication. We give the final expression for the resulting free energy:

$$\begin{aligned} \Omega = & -T \sum_k \log(1 + e^{-\beta(R\tilde{\epsilon}_k R^\dagger + \lambda - \mu)}) \\ & + T \sum_i \text{Tr} \log[1 - e^{-\beta(\hat{H}_{\text{embed}} - E^c \hat{I})}] + E^c \\ & - \sum_{i,\alpha\beta} (\lambda_{\alpha\beta} + \lambda_{\alpha\beta}^c) \Delta_{\alpha\beta}^p \\ & - \sum_{i;\alpha\beta\gamma} (\mathcal{D}_{\alpha\beta} R_{\gamma\alpha} + \text{c.c.}) [\Delta^p (1 - \Delta^p)]_{\gamma\beta}^{1/2}, \quad (\text{C3}) \end{aligned}$$

where \hat{I} is an identity matrix with the size of the Hilbert space of \hat{H}_{embed} .

The fact that DMET is a simplification of RISB with $R = 1$ gives an easy way to generalize DMET to finite temperatures. The implications of this finite-temperature extension of RISB and DMET will be explored in a separate publication.

-
- [1] A. Georges, G. Kotliar, W. Krauth, and M. J. Rozenberg, *Rev. Mod. Phys.* **68**, 13 (1996).
- [2] M. H. Hettler, A. N. Tahvildar-Zadeh, M. Jarrell, T. Pruschke, and H. R. Krishnamurthy, *Phys. Rev. B* **58**, R7475 (1998).
- [3] M. H. Hettler, M. Mukherjee, M. Jarrell, and H. R. Krishnamurthy, *Phys. Rev. B* **61**, 12739 (2000).
- [4] A. I. Lichtenstein and M. I. Katsnelson, *Phys. Rev. B* **62**, R9283 (2000).
- [5] G. Kotliar, S. Y. Savrasov, G. Pálsson, and G. Biroli, *Phys. Rev. Lett.* **87**, 186401 (2001).
- [6] T. A. Maier, M. Jarrell, T. Pruschke, and M. H. Hettler, *Rev. Mod. Phys.* **77**, 1027 (2005).
- [7] G. Rohringer, H. Hafermann, A. Toschi, A. A. Katanin, A. E. Antipov, M. I. Katsnelson, A. I. Lichtenstein, A. N. Rubtsov, and K. Held, *arXiv:1705.00024*.
- [8] C. Gros and R. Valentí, *Phys. Rev. B* **48**, 418 (1993).
- [9] D. Sénéchal, D. Perez, and M. Pioro-Ladrière, *Phys. Rev. Lett.* **84**, 522 (2000).
- [10] M. Potthoff, *Eur. Phys. J. B* **32**, 429 (2003).
- [11] M. Potthoff, in *Strongly Correlated Systems*, edited by A. Avella and F. Mancini, Springer Series in Solid-State Sciences Vol. 171 (Springer, Berlin, 2012).
- [12] D. Zgid and E. Gull, *New J. Phys.* **19**, 023047 (2017).
- [13] T. N. Lan and D. Zgid, *arXiv:1703.06981v1*.
- [14] M. Potthoff, *Phys. Rev. B* **64**, 165114 (2001).
- [15] G. Moeller, Resolving low energy spectral properties in correlated electron systems, Ph.D. thesis, Rutgers University, Piscataway, NJ, 1994.
- [16] E. Fromager, *Mol. Phys.* **113**, 419 (2015).
- [17] B. Senjean, M. Tsuchiizu, V. Robert, and E. Fromager, *Mol. Phys.* **115**, 48 (2016).
- [18] R. Frésard and P. Wölfle, *Int. J. Mod. Phys. B* **06**, 685 (1992).
- [19] F. Lechermann, A. Georges, G. Kotliar, and O. Parcollet, *Phys. Rev. B* **76**, 155102 (2007).
- [20] G. Knizia and G. K.-L. Chan, *Phys. Rev. Lett.* **109**, 186404 (2012).
- [21] G. Knizia and G. K.-L. Chan, *J. Chem. Theory Comput.* **9**, 1428 (2013).
- [22] M. Ferrero, P. S. Cornaglia, L. De Leo, O. Parcollet, G. Kotliar, and A. Georges, *Europhys. Lett.* **85**, 57009 (2008).
- [23] M. Ferrero, P. S. Cornaglia, L. De Leo, O. Parcollet, G. Kotliar, and A. Georges, *Phys. Rev. B* **80**, 064501 (2009).
- [24] I. I. Mazin, H. O. Jeschke, F. Lechermann, H. Lee, M. Fink, R. Thomale, and R. Valentí, *Nat. Commun.* **5**, 4261 (2014).
- [25] N. Lanatà, H. U. R. Strand, X. Dai, and B. Hellsing, *Phys. Rev. B* **85**, 035133 (2012).
- [26] J. I. Facio, V. Vildosola, D. J. García, and P. S. Cornaglia, *Phys. Rev. B* **95**, 085119 (2017).
- [27] C. Piefke and F. Lechermann, *arXiv:1708.03191*.
- [28] N. Lanatà, Y. X. Yao, C. Z. Wang, K. M. Ho, and G. Kotliar, *Phys. Rev. X* **5**, 011008 (2015).
- [29] N. Lanatà, Y. Yao, X. Deng, V. Dobrosavljević, and G. Kotliar, *Phys. Rev. Lett.* **118**, 126401 (2017).
- [30] G. Kotliar and A. E. Ruckenstein, *Phys. Rev. Lett.* **57**, 1362 (1986).
- [31] J. Bünenmann and F. Gebhard, *Phys. Rev. B* **76**, 193104 (2007).
- [32] B.-X. Zheng and G. K.-L. Chan, *Phys. Rev. B* **93**, 035126 (2016).
- [33] B.-X. Zheng, J. S. Kretchmer, H. Shi, S. Zhang, and G. K.-L. Chan, *Phys. Rev. B* **95**, 045103 (2017).
- [34] I. W. Bulik, G. E. Scuseria, and J. Dukelsky, *Phys. Rev. B* **89**, 035140 (2014).
- [35] S. Wouters, C. A. Jiménez-Hoyos, Q. Sun, and G. K. Chan, *J. Chem. Theory Comput.* **12**, 2706 (2016).
- [36] S. Wouters, C. A. Jiménez-Hoyos, and G. K. L. Chan, *arXiv:1605.05547*.

- [37] A. Isidori and M. Capone, *Phys. Rev. B* **80**, 115120 (2009).
- [38] G. Mazza and A. Georges, *Phys. Rev. B* **96**, 064515 (2017).
- [39] G. H. Booth and G. K.-L. Chan, *Phys. Rev. B* **91**, 155107 (2015).
- [40] M. Schiró and M. Fabrizio, *Phys. Rev. Lett.* **105**, 076401 (2010).
- [41] M. Schiró and M. Fabrizio, *Phys. Rev. B* **83**, 165105 (2011).
- [42] N. Lanatà and H. U. R. Strand, *Phys. Rev. B* **86**, 115310 (2012).
- [43] G. Mazza and M. Fabrizio, *Phys. Rev. B* **86**, 184303 (2012).
- [44] M. Behrmann, M. Fabrizio, and F. Lechermann, *Phys. Rev. B* **88**, 035116 (2013).
- [45] G. Mazza, A. Amaricci, M. Capone, and M. Fabrizio, *Phys. Rev. B* **91**, 195124 (2015).
- [46] M. Behrmann and F. Lechermann, *Phys. Rev. B* **91**, 075110 (2015).
- [47] J. S. Kretchmer and G. K.-L. Chan, [arXiv:1609.07678v1](https://arxiv.org/abs/1609.07678v1).
- [48] J. Kolorenč, A. I. Poteryaev, and A. I. Lichtenstein, *Phys. Rev. B* **85**, 235136 (2012).
- [49] J. Kolorenč, A. B. Shick, and A. I. Lichtenstein, *Phys. Rev. B* **92**, 085125 (2015).
- [50] M. Caffarel and W. Krauth, *Phys. Rev. Lett.* **72**, 1545 (1994).
- [51] I. W. Bulik, Electron correlation in extended systems via quantum embedding, Ph.D. thesis, Rice University, Houston, Texas, 2015.
- [52] S. Onoda and M. Imada, *Phys. Rev. B* **67**, 161102 (2003).
- [53] A. Avella and F. Mancini, *Eur. Phys. J. B* **50**, 527 (2006).
- [54] D. Jacob, K. Haule, and G. Kotliar, *Phys. Rev. B* **82**, 195115 (2010).
- [55] N. Lin, C. A. Marianetti, A. J. Millis, and D. R. Reichman, *Phys. Rev. Lett.* **106**, 096402 (2011).